

AD-786 380

**TURBULENT BOUNDARY LAYER AND VISCOUS  
RESISTANCE OF A SUBMARINE AT HIGH REYNOLDS  
NUMBER**

**William G. Souders**

**Naval Ship Research and Development Center  
Bethesda, Maryland**

**May 1974**

**DISTRIBUTED BY:**

**NTIS**

**National Technical Information Service  
U. S. DEPARTMENT OF COMMERCE  
5285 Port Royal Road, Springfield Va. 22151**

UNCLASSIFIED

SECURITY CLASSIFICATION OF THIS PAGE (When Data Entered)

REPORT DOCUMENTATION PAGE		READ INSTRUCTIONS BEFORE COMPLETING FORM
1. REPORT NUMBER 4366	2. GOVT ACCESSION NO.	3. RECIPIENT'S CATALOG NUMBER AD 786 380
4. TITLE (and Subtitle) TURBULENT BOUNDARY LAYER AND VISCOUS RESISTANCE OF A SUBMARINE AT HIGH REYNOLDS NUMBER		5. TYPE OF REPORT & PERIOD COVERED
7. AUTHOR(s) William G. Souders		6. PERFORMING ORG. REPORT NUMBER
9. PERFORMING ORGANIZATION NAME AND ADDRESS Naval Ship Research and Development Center Bethesda, Md. 20034		8. CONTRACT OR GRANT NUMBER(s)
11. CONTROLLING OFFICE NAME AND ADDRESS Naval Ship Systems Command Washington, D. C. 20360		10. PROGRAM ELEMENT, PROJECT, TASK AREA & WORK UNIT NUMBERS (See reverse side)
12. REPORT DATE May 1974		13. NUMBER OF PAGES 30
14. MONITORING AGENCY NAME & ADDRESS (if different from Controlling Office)		15. SECURITY CLASS. (of this report) UNCLASSIFIED
		15a. DECLASSIFICATION/DOWNGRADING SCHEDULE
16. DISTRIBUTION STATEMENT (of this Report)  APPROVED FOR PUBLIC RELEASE: DISTRIBUTION UNLIMITED		
17. DISTRIBUTION STATEMENT (of the abstract entered in Block 20, if different from Report)		
18. SUPPLEMENTARY NOTES		
19. KEY WORDS (Continue on reverse side if necessary and identify by block number)  Reproduced by NATIONAL TECHNICAL INFORMATION SERVICE U S Department of Commerce Springfield VA 22151		
20. ABSTRACT (Continue on reverse side if necessary and identify by block number) A limited amount of data about turbulent boundary layers, obtained on a full-scale submarine, is presented. Mean wall-shear stresses were measured at four hull locations with Preston tubes, and mean velocity profiles in the boundary layer were measured at one hull location with pitot tubes. These measurements were made over a range of Reynolds numbers from $1.91 \times 10^7$ to $3.05 \times 10^8$ . The measured profile for boundary-layer velocity, both full-scale and model, agree well with the velocity-similarity laws, and the measurements of shear-stress distribution are in agreement with a solution of the momentum equation for a body of revolution.		

DD FORM 1 JAN 73 1473

EDITION OF 1 NOV 65 IS OBSOLETE  
S/N 0102-014-6601

UNCLASSIFIED

SECURITY CLASSIFICATION OF THIS PAGE (When Data Entered)

**UNCLASSIFIED**

SECURITY CLASSIFICATION OF THIS PAGE(When Data Entered)

(Block 10)

Subproject SF 35421003

Task 01710

Element 62512N

Work Unit 1-1508-305

Task SR 0230101

Work Unit 1-1556-032

**UNCLASSIFIED**

SECURITY CLASSIFICATION OF THIS PAGE(When Data Entered)

## TABLE OF CONTENTS -

	Page
ABSTRACT . . . . .	1
ADMINISTRATIVE INFORMATION . . . . .	1
INTRODUCTION . . . . .	1
ANALYTICAL BACKGROUND . . . . .	2
VELOCITY-SIMILARITY LAWS . . . . .	3
Laminar Sublayer . . . . .	3
Inner Law or Law of the Wall . . . . .	4
Outer Law or Velocity-Defect Law . . . . .	4
DETERMINATION OF WALL SHEAR STRESS . . . . .	4
Preston Tube . . . . .	4
Stanton Tube . . . . .	5
Logarithmic Velocity Law . . . . .	6
THE EXPERIMENTAL VEHICLE . . . . .	6
SHIP GEOMETRY . . . . .	6
PREPARATION OF HULL . . . . .	6
METHOD AND PROCEDURES . . . . .	8
PRESSURE TUBES . . . . .	8
Rake and Pitot Tubes . . . . .	8
Pitot Tube Rake Corrections . . . . .	10
Static Pressure Measurements . . . . .	11
Stanton and Preston Tubes . . . . .	11
DATA COLLECTION . . . . .	12
Pressure Transducers and Electronic Instrumentation . . . . .	12
Pressure Transducer Calibration . . . . .	14
Ship Speed Log . . . . .	14
TRIAL PROCEDURE . . . . .	14
RESULTS AND DISCUSSION . . . . .	16
MEAN VELOCITY PROFILES . . . . .	16
WALL SHEAR STRESS . . . . .	18
CONCLUSIONS . . . . .	19
REFERENCES . . . . .	21

## LIST OF FIGURES

	Page
1 – Submarine Hull Shape, Showing Pressure-Probe Locations . . . . .	7
2 – Boundary Layer–Mean Velocity–Profile Rake . . . . .	9
3 – Surface-Tube Installation in Mounting Plate . . . . .	13
4 – Valving Arrangement of Pressure Transducer . . . . .	13
5 – Electronic Instrumentation . . . . .	15
6 – Outer Law or Velocity-Defect Law . . . . .	15
7 – Inner Law or Law of the Wall . . . . .	17
8 – Variation of Wall Shear-Stress Coefficient along the Keel for Various Ship Speeds . . . . .	17
9 – Displacement of Effective Center for Stanton Tubes . . . . .	20
10 – A Typical Stanton Tube Calibration Curve: Variation of Hull Shear Stress as a Function of Stanton Tube Differential Pressure -- $l = 17$ Feet . . . . .	20

## NOTATION

A	Slope of inner logarithmic velocity law for ordinary Newtonian fluid or $2.3026/K$ , Equation (3)
$a_i$	Coefficients of sixth degree polynomial defining ship meridian profile, $i = 0, 5$
B	Constant of ordinary Newtonian inner logarithmic velocity law, Equation (3)
$c_\tau$	Wall shear stress coefficient, $c_\tau = \tau_w / \rho U^2$
D	Maximum diameter of ship hull
$d_p$	Preston tube outside diameter
$d_s$	Height of Stanton tube above wall
$\bar{d}_s$	Deviation of effective center of Stanton tube from geometric center
K	von Kármán constant, Equation (3)
L	Length of ship
$\ell$	Axial distance along ship
q	Dynamic pressure, $q = 1/2 \rho u^2$
$R_\ell$	Reynolds number based on $\ell$ , $R_\ell = U_\infty \ell / \nu$
$R_x$	Reynolds number, based on $x$ , $R_x = U_\infty x / \nu$
$r_w$	Radial distance from ship-profile axis to hull
U	Mean velocity at the outer edge of the boundary layer
$U_\infty$	Ship speed
u	Local mean velocity in direction of flow
$u_\tau$	Shear velocity, $u_\tau = \sqrt{\tau_w / \rho}$
$u^+$	$u / u_\tau$
x	Distance along the meridian from the bow

$x^*$	$\log_{10} (\Delta P_p d_p^2 / 4 \rho \nu^2)$
$y$	Normal distance from the wall
$y_\ell$	Thickness of the laminar sublayer, Equation (1)
$y_\ell^+$	Nondimensional thickness of laminar sublayer, $y_\ell^+ \equiv \frac{u_\tau y_\ell}{\nu}$
$y^+$	Nondimensional distance from the wall, $y^+ \equiv u_\tau y / \nu$
$y^*$	$\log_{10} (\tau_w d_p^2 / 4 \rho \nu^2)$
$\Delta P_p$	Preston tube dynamic pressure
$\Delta P_s$	Stanton tube dynamic pressure
$\delta$	Boundary layer thickness
$\nu$	Kinematic viscosity of the fluid
$\rho$	Density of fluid
$\tau_w$	Wall shear stress
$\Omega$	Coles wake parameter, Equation (4)

## ABSTRACT

A limited amount of data about turbulent boundary layers, obtained on a full-scale submarine, is presented. Mean wall-shear stresses were measured at four hull locations with Preston tubes, and mean velocity profiles in the boundary layer were measured at one hull location with pitot tubes. These measurements were made over a range of Reynolds numbers from  $1.91 \times 10^7$  to  $3.05 \times 10^8$ .

The measured profile for boundary-layer velocity, both full-scale and model, agree well with the velocity-similarity laws, and the measurements of shear-stress distribution are in agreement with a solution of the momentum equation for a body of revolution.

## ADMINISTRATIVE INFORMATION

The research presented in this paper was authorized by the Naval Ship Systems Command. Funding was provided under Subproject SF 35421003, Task 01710, Element 62512N, Work Unit 1-1508-305. Data analysis and report preparation were authorized and funded by the Naval Ship Research and Development Center under its General Hydromechanics Research Program, Task SR 0230101, Work Unit 1-1556-032.

## INTRODUCTION

Streamlined axisymmetric bodies have important practical naval application to underwater missiles and, more important, submarine hulls. Any knowledge of the development of the turbulent boundary layer on these bodies, especially at high Reynolds numbers, would be valuable in designing submarine hull appendages, openings and propellers operating in the wakes. In addition, experimental data about the local flow along such bodies can aid in formulating and confirming methods for calculating the frictional resistance of these bodies.

Most experimental studies dealing with turbulent boundary layer flows at high Reynolds numbers are limited to smooth flat plates.<sup>1-4</sup> Few of these studies are in the practical Reynolds number range of ship boundary layers. Model studies of the boundary layer on a body of revolution at relatively low Reynolds numbers indicate that the local wall shear stress along a body of revolution when compared to that of a flat plate is higher over the forward portion and lower over the after portion of the body. During the fall of 1957 an extensive

---

<sup>1</sup>Hama, F. R., "Boundary-Layer Characteristics for Smooth and Rough Surfaces," Transactions of the Society of Naval Architects and Marine Engineers, Vol. 62, p. 333 (1954). A complete list of references is given on page 21.

<sup>2</sup>Schoenherr, K. E., "Resistance of Flat Surfaces Moving through a Fluid," Transactions of the Society of Naval Architects and Marine Engineers, Vol. 40, p. 279 (1932).

<sup>3</sup>Schultz-Grunow, F., "New Frictional Resistance Law for Smooth Plates," National Advisory Committee for Aeronautics Technical Memorandum 986 (1941); Translation from Luft-fahrtforschung (1940).

<sup>4</sup>Granville, P. S., "The Viscous Resistance of Surface Vessels and the Skin Friction of Flat Plates," Transactions of the Society of Naval Architects and Marine Engineers, Vol. 64 (1956).

boundary-layer survey was conducted on a full-scale submarine, a well-streamlined body of revolution. Velocity profiles and wall shear stresses were measured over speeds ranging from 16.9 to 33.7 feet per second at 14 stations on the hull. Due to limitations in the electronic instrumentation, the boundary-layer velocity and wall shear-stress data were presented as averages over the range of ship speeds. In general, the trends of these composite data were similar to trends predicted by existing boundary-layer theories. Theoretical investigations of the turbulent boundary layer on bodies of revolution include work by von Kármán,<sup>5</sup> Young and Owen,<sup>6</sup> and Granville.<sup>7</sup>

In the spring of 1968 extensive full-scale trials were authorized on a full-scale submarine. This authorization presented an opportunity to obtain a limited amount of boundary-layer data at full-scale Reynolds numbers.

This reports presents the results of the boundary-layer measurements which encompassed mean velocity profiles at one station, using pitot tubes and mean wall-shear stresses at four longitudinal stations, using Preston surface tubes. These measurements at full scale were made fully submerged at a 250-ft keel depth over a full range of ship speeds from 16.9 to 33.7 feet per second. The measured profiles for boundary-layer velocity for both full-scale and model ships are compared with the two-dimensional velocity defect law and the law of the wall. The longitudinal shear-stress results obtained from the Preston surface-tube pressure data are also presented.

A Stanton tube was placed beside each of the Preston tubes. Although these tubes were used for another phase of the trails which is not reported here, description and results from the calibrations are given in this report.

## ANALYTICAL BACKGROUND

The following discussion is intended as an introduction to the presentation of the experimental results. The mean velocity profiles are compared to the well-established, velocity-similarity laws based on the three-layer, mean velocity-profile model. The basis for using Preston and Stanton tubes and the regions of the boundary layer where their use is valid are also discussed briefly. The wall shear stress was determined from the measured velocity profiles, using both the slope method and direct Preston tube measurements.

---

<sup>5</sup>von Kármán, T., "On Laminar and Turbulent Friction," National Advisory Committee for Aeronautics TM 1092 (Sep 1946); Translation from ZAMM (Aug 1921).

<sup>6</sup>Young, A. D. and P. R. Owen, "A Simplified Theory for Streamline Bodies of Revolution and its Application to the Development of High-Speed Shapes," Aeronautical Research Committee (Great Britain) R & M 2071 (Jul 1943).

<sup>7</sup>Granville, P. S., "The Calculation of the Viscous Drag of Bodies of Revolution," David Taylor Model Basin Report 849 (Jul 1953).

## VELOCITY-SIMILARITY LAWS

For the two-dimensional flow of a Newtonian fluid, it is well-established<sup>8,9</sup> that the velocity distribution within the turbulent boundary layer can be represented by various logarithmic velocity laws. The three-layer nondimensional velocity profile is valid for both internal and external boundary-layer flows and is described briefly in the following text.

### Laminar Sublayer

The laminar sublayer is the very thin layer of flow in contact with the wall where viscous effects dominate, and turbulent fluctuations are essentially damped out. In this region, the velocity profile is expressed as

$$u^+ \equiv \frac{u}{u_\tau} = \frac{u_\tau y}{\nu} \equiv y^+ \quad 0 \leq y \leq y_\ell \quad (1)$$

where  $u$  = local mean velocity in the direction of flow

$u_\tau$  = shear velocity  $u_\tau = \sqrt{\tau_w/\rho}$

$u^+$  = nondimensional mean velocity  $u^+ = u/u_\tau$

$y$  = normal distance from the wall

$y^+$  = nondimensional distance from the wall  $y^+ = (u_\tau y)/\nu$

$y_\ell$  = thickness of the laminar sublayer

$\nu$  = kinematic viscosity of the fluid

$\rho$  = density of the fluid

$\tau_w$  = wall shear stress.

The nominal thickness of the laminar sublayer  $y_\ell$  is generally considered to be

$$y_\ell^+ \equiv \frac{u_\tau y_\ell}{\nu} \leq 11.6 \quad (2)$$

where  $y_\ell^+$  is the nondimensional thickness of the laminar sublayer. Thus from Equation (2),  $y_\ell$  increases as  $\tau_w$  decreases.

---

<sup>8</sup>Hinze, J. O., "Turbulence," McGraw-Hill Book Company, Inc., New York (1959).

<sup>9</sup>Schlichting, H., "Boundary Layer Theory," McGraw-Hill Book Company, Inc., New York (1960).

### Inner Law or Law of the Wall

This region applies to the flow adjacent to the solid boundary where both viscous and inertial effects are important; this region can be expressed as

$$u^+ = A \log_{10} y^+ + B \quad y_l \leq y \leq 0.2\delta \quad (3)$$

where  $\delta$  = boundary-layer thickness

A = slope of the logarithmic velocity law for ordinary Newtonian fluids  
or  $(2.3026)/K$

K = von Kármán constant

B = constant for the ordinary Newtonian inner logarithmic velocity law.

The values of the two constants A and B are taken from data for Newtonian fluids, A = 5.75, and B = 5.5. The universal value for the von Kármán constant K is taken as 0.4.

### Outer Law or Velocity-Defect Law

At some distance from the wall, where U is the velocity at the outer edge of the boundary layer, the velocity defect (U-u) is independent of viscous effects, and inertial effects dominate. This region can be expressed as

$$\frac{U-u}{u_\tau} = -A \log_{10} (y/\delta) + \frac{\Omega}{K} [1 + \cos \pi(y/\delta)] \quad y_l \leq y \leq \delta \quad (4)$$

where U is the mean velocity at the outer edge of the boundary layer, and  $\Omega$  is the Coles wake parameter. The symbols in the last bracket of the equation are for the Hinze approximate wake function,<sup>8</sup> where  $\pi = 3.1416$ .

## DETERMINATION OF WALL SHEAR STRESS

The wall shear stress  $\tau_w$  or skin friction coefficient  $c_f$  may be determined by direct measurement, using impact tubes set flush with the wall surface. Two such tubes are the Preston and Stanton tubes, which are described in the following paragraphs.

### Preston Tube

The Preston tube<sup>10</sup> is an ordinary pitot tube, mounted directly on the wall and small enough to lie within the inner law region.

---

<sup>10</sup>Preston, J. H., "The Determination of Turbulent Skin Friction by Means of Pitot Tubes," Journal of the Royal Aeronautical Society, Vol. 58 (1954).

The Preston tube-pressure data reported in this paper were converted to shear stress by using a universal calibration given by Patel.<sup>11</sup> An empirical relation which best fits the experimental pipe data is given as

$$x^* = y^* + 2 \log_{10} (1.95 y^* + 4.10) \quad (5)$$

for

$$3.5 < y^* < 5.3$$

or

$$55 < u_\tau d_p / 2\nu < 800$$

where  $x^* \equiv \log_{10} (\Delta P_p d_p^2 / 4 \rho \nu^2)$ , and  $y^* \equiv \log_{10} (\tau_w d_p^2 / 4 \rho \nu^2)$ .

Here  $\Delta P_p$  is the dynamic pressure sensed by the Preston tube, and  $d_p$  is the outside diameter of the Preston tube.

Thus, the Preston tube served to provide both the shear-stress distribution data of the hull and the calibration source for the Stanton tube evaluation.

### Stanton Tube

The Stanton tube is a specially constructed narrow type of impact tube adjusted to lie within the very thin laminar sublayer defined by Equation (1). The relation for the Stanton tube in the laminar sublayer is given by Granville<sup>12</sup> as

$$\frac{\Delta P_s d_s^2}{4 \rho \nu^2} = \frac{1}{2} \left( \frac{\tau_w d_s^2}{4 \rho \nu^2} \right)^2 \left( 1 + \frac{\bar{d}_s}{d_s} \right)^2 \quad (6)$$

where  $\Delta P_s$  = dynamic pressure sensed by the Stanton tube

$d_s$  = height of the Stanton tube above the wall

$\bar{d}_s$  = deviation of effective center of the Stanton tube from geometric center.

The Stanton tube requires calibration in known shear flows in order to determine the displacement effects  $\bar{d}_s$  due to the finite size of the tube.

Reported use of the Stanton tube in the literature is scarce and is limited entirely to air flows. The inclusion of the Stanton tube in this investigation served the purpose of demonstrating the measurement technique only, and no additional boundary-layer data have been obtained.

<sup>11</sup>Patel, V. C., "Calibration of the Preston Tube and Limitations on Its Use in Pressure Gradients," *Journal of Fluid Mechanics*, Vol. 23, Part 1, pp. 185-208 (1965).

<sup>12</sup>Granville, P. S., "The Determination of the Local Skin Friction and the Thickness of Turbulent Boundary Layers from the Velocity Similarity Laws," *International Shipbuilding Progress*, Vol. 7, No. 69 (1960).

## Logarithmic Velocity Law

As an alternate to direct measurement, the wall shear stress  $\tau_w$  can be obtained by using the inner law region of the mean velocity profile of Equation (3). To obtain the shear-stress coefficient  $c_\tau$ , the relations  $u_\tau^2 = \tau_w/\rho$  and  $c_\tau = \tau_w/\rho U^2$  are substituted into Equation (3). When the resulting relation is plotted on semilogarithmic paper ( $u$  versus  $y$ ), it appears as a straight line with  $c_\tau$  as a simple function of the slope.

## THE EXPERIMENTAL VEHICLE

### SHIP GEOMETRY

The submarine hull shape (Figure 1) was based on results obtained from resistance tests on a systematic series of bodies of revolution. The meridian profiles of this series are defined by six-degree polynomials.<sup>13</sup> The coefficients of these polynomials are determined from the following six geometric characteristics of the bodies: nose radius, tail radius, volume, length, maximum diameter, and location of maximum diameter. The meridian profile of the submarine is given by

$$\left(\frac{r_w}{D}\right)^2 = \sum_{i=0}^5 a_i \left(\frac{\ell}{L}\right)^{i+1} \quad (7)$$

where  $r_w$  = radial distance from the ship centerline to the hull  
D = maximum diameter of the hull  
 $\ell$  = axial distance from the ship forward point  
L = length of the ship, 200 feet.

The coefficients of the polynomial that define the meridian profile are:

$a_0 =$	1.000000	$a_3 =$	19.784286
$a_1 =$	1.137153	$a_4 =$	- 16.792534
$a_2 =$	- 10.774885	$a_5 =$	5.645977

### PREPARATION OF HULL

To avoid uncertainties in the development of the turbulent boundary layer due to roughness and other hull irregularities, a special ship drydocking was scheduled 2 weeks before the trial.

---

<sup>13</sup>Landweber, L. and M. Gertler, "Mathematical Formulation of Bodies of Revolution," David Taylor Model Basin Report 719 (1950).

A, B, C, AND E - PRESTON TUBE LOCATIONS  
D - VELOCITY PROFILE RAKE LOCATION

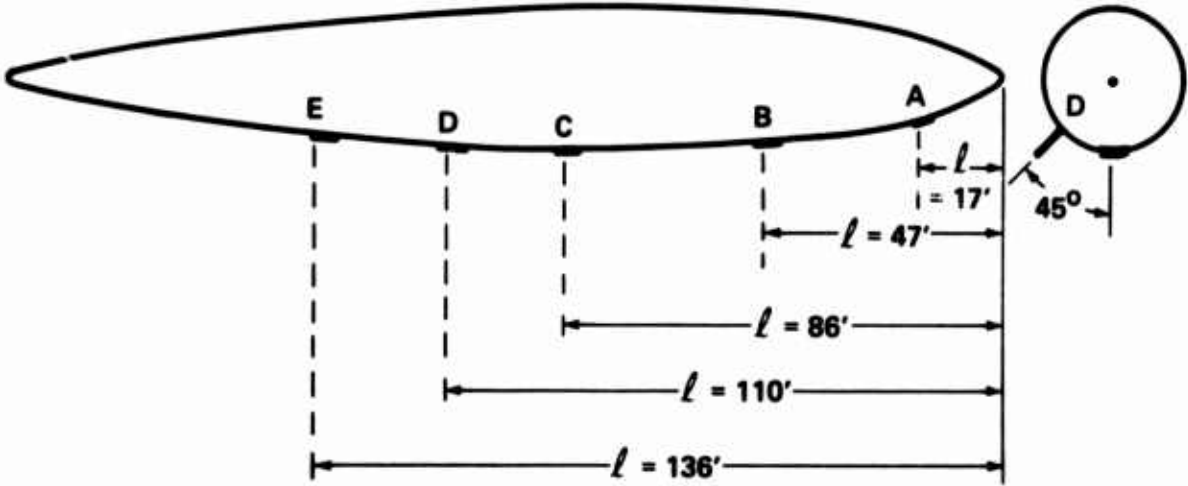


Figure 1 Submarine Hull Shape, Showing Pressure-Probe Locations

To ensure that the submarine hull would be hydrodynamically smooth, it was prepared by using as a guide the specifications given by the Naval Ship Systems Command.<sup>14</sup>

Special care was taken in the area of the surface tubes since excessive hull roughness or marine fouling would result in meaningless data. The intersection of the surface tube-mounting plate, described in the following text, and the hull surface were cleaned to bare metal by power grinders and wire brushes; all resulting grooving and any corrosion pits were covered with vinyl paint and were smoothed with special epoxy compounds. A hull area just forward of each surface-tube plate, approximately 2 feet wide and 6 feet long, received several extra coats of antifouling paint and was smoothed by hand with sandpaper. The surface of the copper nickel insert plate was not painted. The area at the base of the pitot tube rake was also prepared with brushes, grinders, and paint. A rake hull-reference, static pressure tap was drilled in a copper nickel insert plate which was fitted flush into the ship hull, approximately 13 inches forward of the leading edge of the strut. The strut was treated with an antifouling paint having a zinc base. Also, in areas of dissimilar metals, special attention was given to surface preservation to minimize corrosion due to electrolysis.

At the completion of the boundary-layer-survey trials, which covered a 5-month period, the ship was drydocked for removal of rake and equipment. At this time the overall condition of the ship hull was found to be very good. All of the pressure probes of the boundary-layer survey were also in excellent condition; the surface tubes and the pitot tube rake were essentially in the same condition as they were before the trials. The sea water temperature during these trials was between 39° and 47° F, and this probably aided in retarding marine fouling.

## METHOD AND PROCEDURES

### PRESSURE TUBES

All of the experimental equipment described in this section was designed and fabricated at the Naval Ship Research and Development Center. The Portsmouth Naval Shipyard (PTSMH) assisted the Center with shipboard installation and installed all the interconnecting piping between the pressure probes and the recording stations.

### Rake and Pitot Tubes

The boundary-layer, mean velocity profile was measured by using a pitot tube rake (Figure 2), located an axial distance  $l$  of 110 feet from the bow. To avoid the nonaxisymmetric effects of the submarine fairwater and deck, the rake was mounted on the starboard side in

---

<sup>14</sup>Naval Ship Systems Command, "Preservation of Ships in Service," NAVSHIPS Technical Manual 0901-109-002, Chapter 9090.

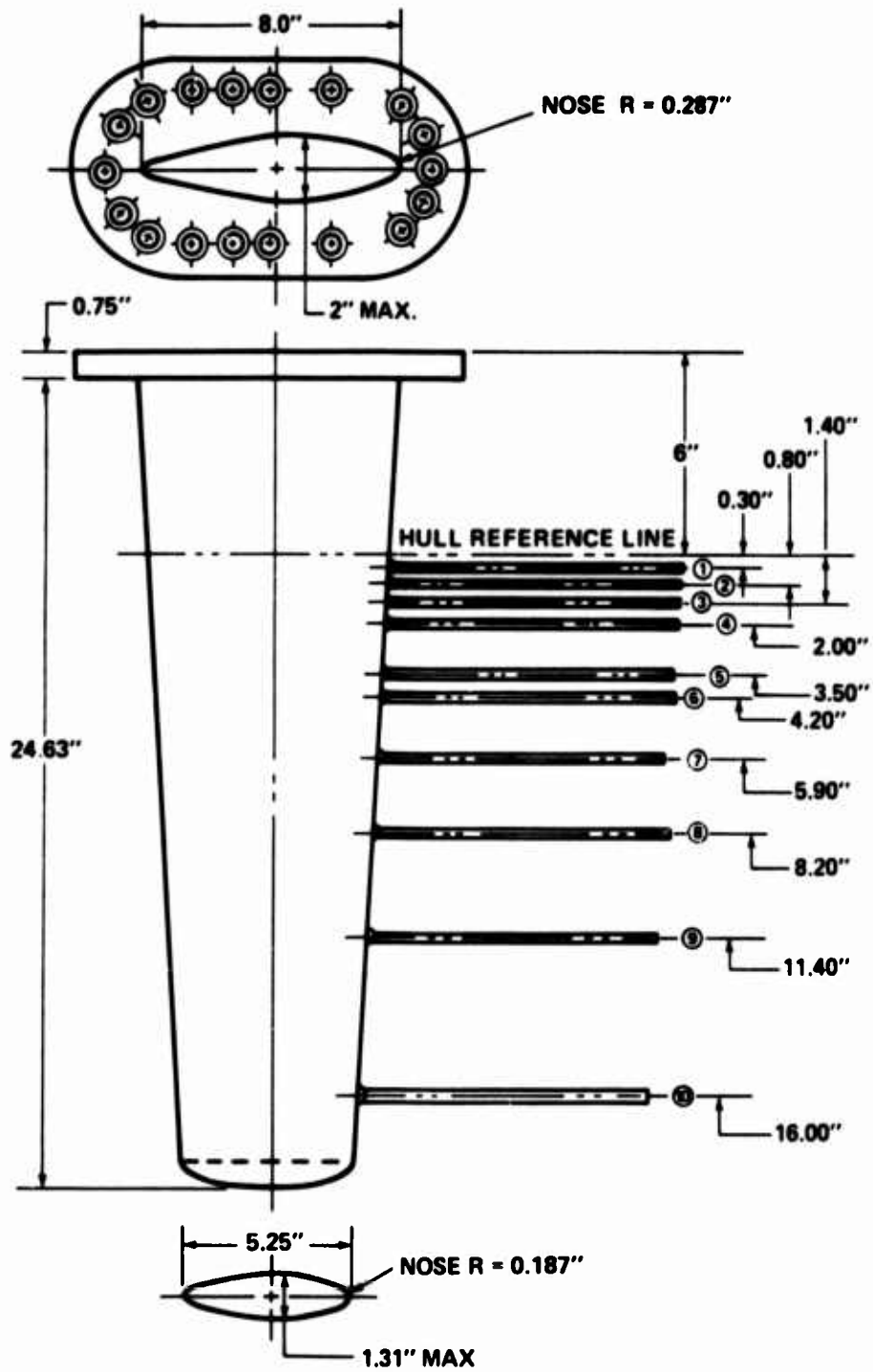


Figure 2 Boundary Layer Mean Velocity Profile Rake

the lower quadrant of the ship, approximately  $45^\circ$  off the keel. The location of the rake on the submarine hull is shown in Figure 1.

The rake strut had a cross section of 4:1 EPH (ellipse-parabola-hyperbola) with a root chord length and thickness of 8.0 and 2.0 inches, respectively, and a tip chord length and thickness of 5.25 and 1.31 inches, respectively. The overall strut length was 24.63 inches. The rake pitot tubes were screwed into the leading edge of the strut. There were 10 9-inch-long pressure tubes; the 9 innermost tubes were total head-type pitot tubes with outer diameters of  $3/16$  inch and the outermost tube was a pitot static tube with an outer diameter of  $3/8$  inch. All of the pressure tubes had elliptical nose sections. The distances of the pressure tubes from the ship hull are given in Figure 2. An additional static pressure was obtained from two common piezometer taps in the hull near the projected tip of the pitot tubes.

The design of the boundary layer-mean velocity-profile rake was guided primarily by past experimental results obtained from submarine boundary-layer-survey trials conducted in the fall of 1957. Boundary-layer thickness and velocity-profile data were aids in determining geometries of strut and pitot tube. All of the pitot tubes were designed to be located well within the ship boundary layer, except for the outermost tube, which was located just outside the boundary layer. Most of the pitot tubes were closely grouped in the area near the hull in order to obtain the maximum possible definition of the law of the wall region  $y_0 \leq y \leq 0.2\delta$ .

### Pitot Tube Rake Corrections

A review of possible sources of errors inherent in using a pitot tube rake to measure velocities in shear flows indicated that resulting corrections would be less than the experimental accuracy; thus, the data are presented without correction. However, a brief discussion follows about some of the possible sources of error that were considered:

1. Extraneous pressure fields due to the presence of the strut
2. Small misalignment of the rake or pitot tube
3. Other impact tube-interference effects.

To determine effects due to pressure fields and/or small misalignments, the pitot tube rake was calibrated in the high-speed basin at the Center before the trials. The tests were run at speeds ranging from 16.9 to 33.7 fps with the strut at  $0^\circ$  and  $5^\circ$  angles of yaw. The geometry was the same as the full-scale installation—pitot tubes, static holes, etc.—except that a flat surface plate was used to simulate the ship hull. All the pitot tubes were outside the plate boundary layer and therefore sensed carriage speed. The velocities indicated by all the pitot tubes were within 1.5 percent of the carriage velocity. Since they included data from both strut angles of attack,  $0^\circ$  and  $5^\circ$ , it was considered that small misalignments of the strut would not be serious.

Other impact tube-interference effects investigated were the displacement effect due to shear flow, wall effect, and turbulence. It was concluded that any possible corrections from these sources would not substantially affect the present trial results. These effects are discussed in References 15-17.

### Static Pressure Measurements

When velocity measurements are made with an impact tube, the static pressure taps should be as close as possible to the impact tube. When feasible, a good way to accomplish this is through the use of pitot static tubes. In the present experiments, however, it was essential to obtain the maximum possible definition of the velocity in the law of the wall region. Therefore, it was decided to use impact tubes on the rake because a smaller diameter could be achieved at reasonable cost. The exception was the outermost tube on the rake: a pitot static tube was used there because size was not a problem. In addition, a pair of common static holes was installed in the ship hull at the same longitudinal position as the impact-tube opening. Thus, the static pressure could be measured at the outermost pitot static tube and on the ship hull. Both static pressure sources could be used individually or in combination, and it was possible to monitor any difference between the two pressures. This difference was recorded throughout the trial and was found to be negligible.

### Stanton and Preston Tubes

To measure the longitudinal shear stress distribution on the hull, Preston tubes were installed at four stations along the keel at  $x$  of 17, 47, 86, and 136 feet from the bow. The location of these tubes on the submarine hull is shown in Figure 1.

The Preston tubes were mounted directly on the hull and were small enough, 0.065 in OD and 0.037 in ID, to lie within the inner law region. These tubes had square cut ends and were made of stainless steel.

The Stanton tubes were specially constructed, total-head-type impact tubes: they were located next to the Preston tubes and were sufficiently small to lie within the very thin laminar sublayer; see Equation (1). The conceptual design of the Stanton tube was obtained from Head and Rechnerberg.<sup>18</sup> Its top consisted of 0.002-inch-thick shim stock, which was

---

<sup>15</sup>Daily, J. W. and R. L. Hardison, "A Review of Literature Concerning Impact Probes Used in Steady Flows." Massachusetts Institute of Technology Hydrodynamics Laboratory Report 67, Appendix 1 (Apr 1964).

<sup>16</sup>MacMillan, F. A., "Experiments on Pitot-Tubes in Shear Flow," Aeronautical Research Committee Reports and Memoranda 3028 (Feb 1956).

<sup>17</sup>Scotton, V. E., "Turbulent Boundary Layer Characteristics over a Rough Surface in an Adverse Pressure Gradient," NSRDC Report 2659 (1967).

<sup>18</sup>Head, M. R. and I. Rechnerberg, "The Preston Tube as a Means of Measuring Skin Friction," *Journal of Fluid Mechanics*, Vol. 14, Part 1, pp. 1-17 (1962).

ground to a knife edge and was adjusted to be 0.0015 inch above the ship hull. The ship hull formed the lower boundary of the tube. Both the Preston and Stanton tubes were built into a 9-inch-diameter, copper nickel plate which was carefully fitted flush with the ship hull; see Figure 3. The static reference pressure for both impact tubes was provided by a 1/32-inch-diameter, static pressure portal, located 1 1/2 inches from them. A coverplate protected the surface tubes during drydocking periods and independent ship exercises before the full-scale trials and were removed by divers before the experiment.

## **DATA COLLECTION**

### **Pressure Transducers and Electronic Instrumentation**

The pressures from the boundary-layer probes were sensed by variable reluctance pressure transducers (Validyne Model DP 15-560). Their full-scale differential pressures ranged from 0.1 to 500 psid, depending on the diaphragm used. Full-scale values from 0.2 to 25.0 psi were used for this investigation. The rated linearity and hysteresis of the transducer is 0.5 percent, full scale. The interchangeable diaphragm feature of the Validyne transducer permitted pressures to be measured near the full-scale value of the diaphragm, thus increasing the accuracy obtainable for the measurement.

Each pressure transducer was compactly mounted in a modular switching unit comprised of toggle valves and manifolds. Two types of modules (Figure 4) were used. Module 1 was for pressure probes that had an individual static reference pressure, i.e., Preston and Stanton surface tubes. Module 2 was for pressure probes that utilized a common static reference pressure, i.e., rake pitot tubes. A provision was made for measuring the differential pressure between the hull-surface static pressure taps, located at the base of the rake, and the static pressure portal on the outermost rake pitot static tube. Either or both, an average, of these static pressure sources could be used as a reference pressure for all of the rake pitot tubes. The proper valve arrangement enables the transducer modules to provide the following functions:

1. "Bleeding" or flushing air bubbles trapped in the pressure lines and transducer
2. Flushing pressure lines back to the sea to remove foreign particles and fouling deposits from the pressure probe inlets
3. Zero differential pressure across the transducer when the ship was in motion
4. A means of transducer calibration, using the manifolds
5. Collecting pressure data and isolating a pressure transducer from the rest of the system at any time.

The analog signals from the pressure transducers were conditioned with a carrier demodulator amplifier (NSRDC Type 594-1A AC) and were filtered with low-pass filters

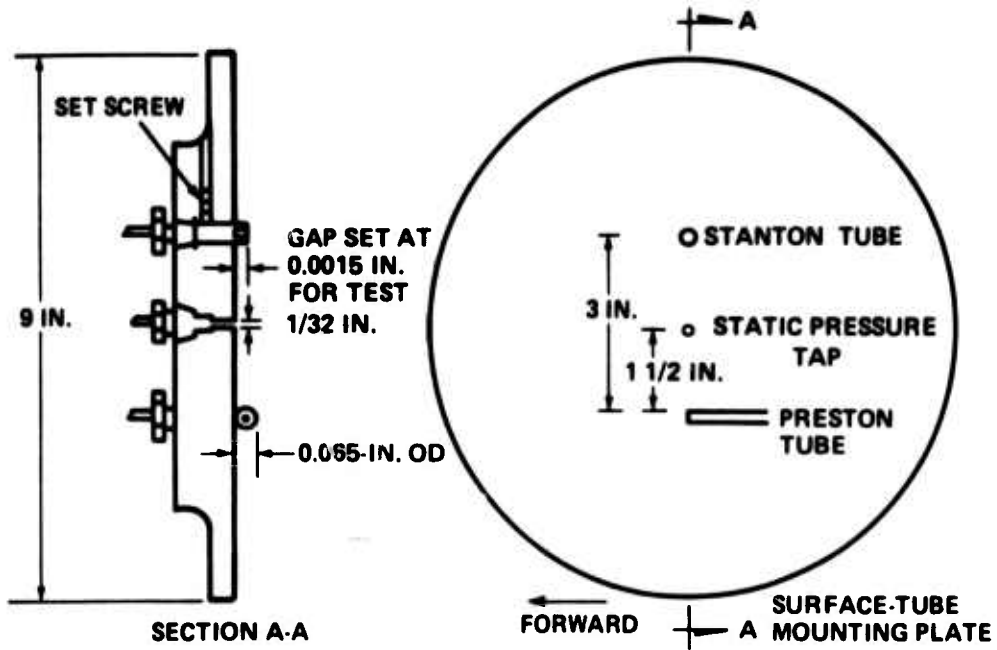


Figure 3 – Surface-Tube Installation in Mounting Plate

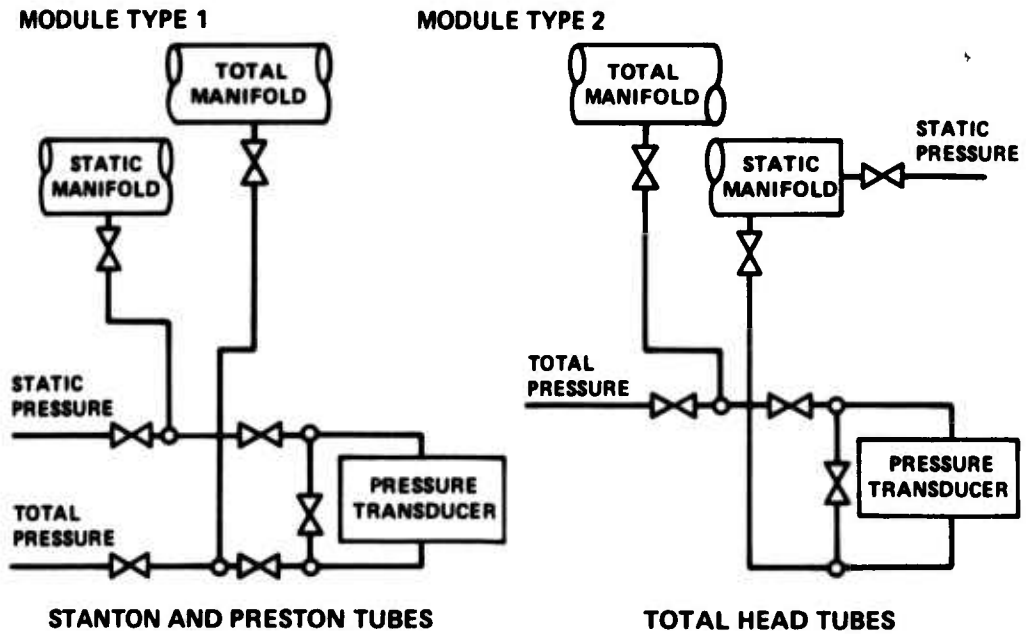


Figure 4 – Valving Arrangement of Pressure Transducer

(NSRDC Type 583). The filtered signal was then processed by an integrating digital voltmeter and printer (VIDAR Model 521). There were 19 electronic channels, 8 for the surface tubes, 10 for the rake pitot tubes, and 1 for the measurement of static pressure difference between the hull static and the pitot static tube. Figure 5 shows the electronic instrumentation.

### **Pressure Transducer Calibration**

Before the boundary-layer trials, the Validyne pressure transducers were calibrated aboard the ship in the same configuration as used for data collection, i.e., by using the shipboard cabling and the electronic instrumentation. A universal electromanometer unit (Consolidated Electrodynamics) was used as the calibration source. It consisted basically of two parts: a transducer or precision pressure balance which operated on the nondisplacement force-balance principle, and a servoamplifier. To cover the range of pressures anticipated for the trials, two precision pressure balances were used during the calibration with full-scale ranges of  $\pm 30$  and  $\pm 5$  pounds per square inch differential. Both pressure balances have an accuracy of 0.05 percent of full scale but can be used only with dry, noncorrosive gas media. The transducer-calibration data were fitted to a straight line by the least square procedure; all of the pressure transducers were within the manufacturer specified accuracy of 0.5 percent, full scale. A similar transducer calibration, performed at the completion of the boundary-layer-survey trials, indicated that the post-trial calibration data agreed well with the pre-trial calibrations, except for results from the lower range diaphragms from 0.2 to 1.5 pounds per square inch. The latter results were within 2 to 4 percent of the pre-trial calibrations. A post-trial examination of these stainless steel diaphragms revealed a slight saltlike crystalline deposit on the diaphragms. This could explain the difference in the two calibrations since the post-calibration data were still linear but of a lower sensitivity.

### **Ship Speed Log**

Ship speeds were obtained from an electromagnetic speed indicator, mounted at the tip of a strut, located approximately 65 ft from the bow in the lower quadrant of the ship. The strut was 20 inches long, enough so that the speed indicator was outside the boundary layer. Before the boundary-layer-survey trials, the speed log was calibrated over the 1/2-mile course at Provincetown, Mass.

### **TRIAL PROCEDURE**

The boundary-layer-survey trial was conducted in the Gulf of Maine during the winter of 1971. The ship was prepared for the trials at PTSMH. All of the boundary-layer-survey trials to be described were conducted with the submarine at  $0^\circ$  angle of attack to ensure axisymmetric flow conditions.

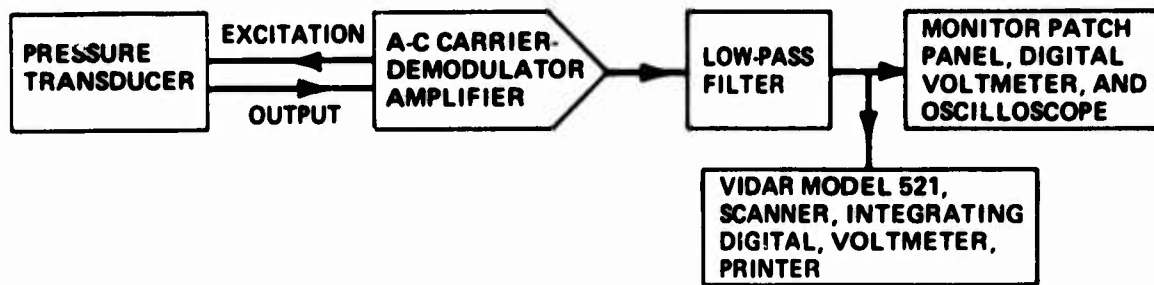


Figure 5 Electronic Instrumentation

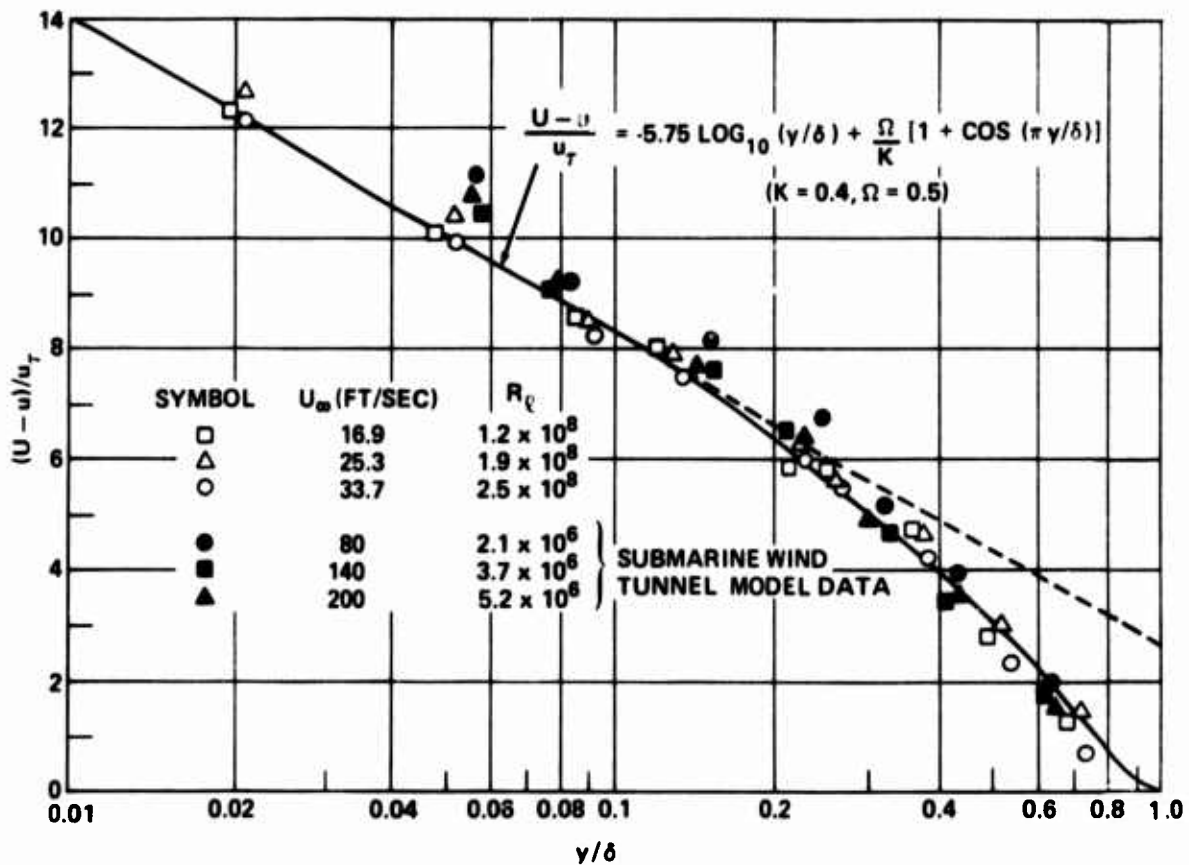


Figure 6 Outer Law or Velocity-Defect Law

The first portion of the trial was conducted over a measured 1/2-mile course in order to calibrate the ship electromagnetic (EM) speed log. Runs were made at periscope depth, 50 feet to keel, over a range of speeds from 13.5 to 27.0 feet per second. A deeply submerged calibration of the EM log was conducted at a keel depth of 250 feet over a full range of shaft revolutions per minute. A limited amount of boundary-layer-pressure data was obtained at this time. The remainder of the trial was then conducted with total data acquisition at ship speeds ranging from 16.9 to 33.7 feet per second with the ship submerged at a 250-foot keel depth.

The procedure for the data collection runs was as follows. The ship was steadied on course, speed, and depth. After a 30-sec standby period, the ship made a 1-min approach under steady-state conditions, followed by 3 min of data recording.

Each of the 19 pressure data channels was recorded continuously from the beginning of the approach period to the end of the run at the rate of approximately one digital data sample per 6 seconds. The temperature of the ambient seawater was recorded at test depth by the ship bathythermograph.

## RESULTS AND DISCUSSION

The boundary layer characteristics are presented in two sets of curves; the first contains the results of the mean velocity-profile measurements, and the second gives results of the wall shear-stress distribution. A limited amount of Stanton tube data is also presented.

### MEAN VELOCITY PROFILES

The mean velocity-profile data are compared with the velocity-similarity laws in Figures 6 and 7. The data from several representative profiles are compared with both the velocity-defect law of Equation (4) and the law of the wall of Equation (3). The profiles selected for presentation were chosen to provide the maximum range in the hull shear stress  $\tau_w$  and Reynolds number. The results shown in these figures were measured at ship speeds  $U_\infty$  from 16.9 to 33.7 feet per second, representing a Reynolds number  $R_\ell$  range of approximately  $1.23 \times 10^8$  to  $2.45 \times 10^8$ , based on  $\ell$  from the bow.

The  $\tau_w$  values presented in the data of Figures 6 and 7 were obtained by using the slope method described earlier. The method employed is subject to error because the shear-stress coefficient is sensitive to the slope of a straight line defined by a small number of points, in this case, four or five. However, the values obtained with the rake at  $\ell = 110$  feet were in good agreement with the values of shear stress obtained with the Preston tubes at  $\ell = 86$  and 136 feet. This agreement, together with the agreement of the data with the law of the wall, discussed as follows, gave confidence in the values of  $\tau_w$  obtained by the slope method.

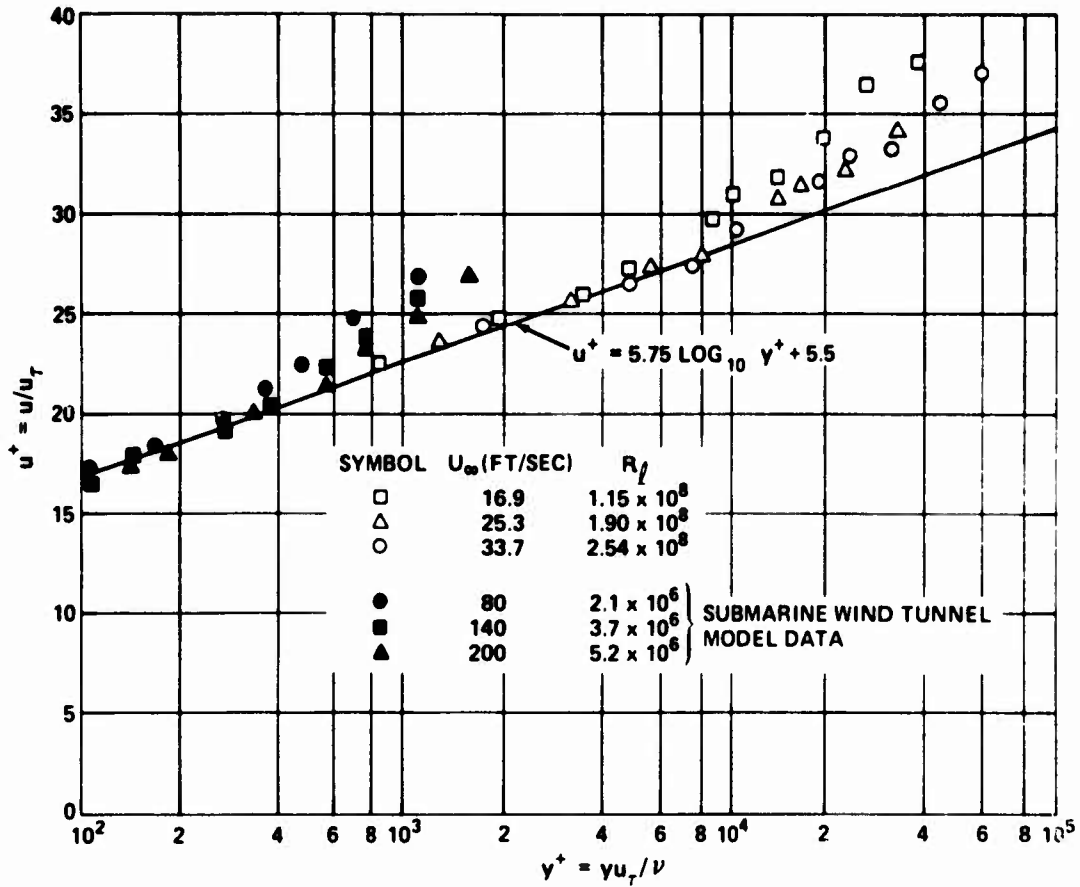


Figure 7 Inner Law or Law of the Wall

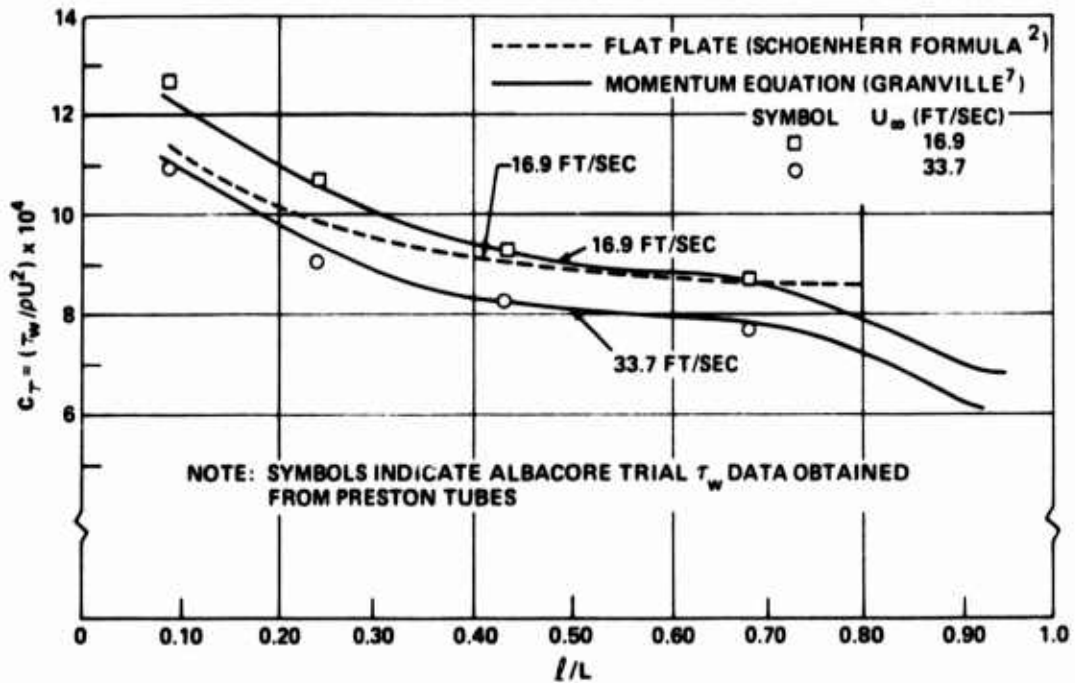


Figure 8 Variation of Wall Shear-Stress Coefficient along the Keel for Various Ship Speeds

The values of  $\delta$  used in Figure 6 were derived by fitting the profile data to a polynomial by a least square fit; the procedure was to set  $u/U = 0.99$  and solve for  $y$ . In general, exact determination of boundary-layer thickness  $\delta$  is difficult, i.e., the point where the boundary-layer flow gradually merges with the external flow. For the subject trials, this difficulty was compounded because (1) for fixed  $\ell$ , the change in  $\delta$  is small over the range of trial ship speeds  $U_\infty$ ; (2) the velocity profile was not well-defined at the outer edge of the boundary layer. An average value of  $\delta = 14.5$  inches was calculated over the range of trial ship speeds at  $\ell = 110$  feet. This value of  $\delta$  is in fair agreement with the empirical relation of Granville<sup>12</sup> for flat plates at high Reynolds number. This relation is given as

$$\frac{\delta}{x} = \frac{0.0598}{\text{Log}_{10} R_x - 3.170} \quad (8)$$

where  $x$  is the distance along the meridian from the bow, and  $R_x = U_\infty x / \nu$ .

For fixed  $x$ , and a  $U_\infty$  range from 16.3 to 33.7 feet per second, Equation (8) gives a corresponding range in  $\delta$  from 16.6 to 15.1 inches.

Several typical mean velocity profiles are plotted in Figure 6, according to the velocity-defect law. The value of  $\tau_w$  ranged from 0.45 to 1.82 pound per foot squared. The velocity-profile data tend to agree well with the velocity-defect formulation over the range of  $y/\delta$  tested. Data for the submarine model are also included in this figure. The model data were obtained from experiments with a 1/26-scale model, conducted in the subsonic wind tunnel at the Center. Velocity profiles of the model presented in Figure 6 represent values of  $U_\infty = 80, 140,$  and  $200$  feet per second, and were taken at  $\ell/L = 0.55$ . This model value of  $\ell/L$  corresponds to the same location where the full-scale profile data were measured. As seen in the figure, the model velocity-profile data are also in agreement with the velocity-defect law.

Figure 7 shows typical mean velocity-profile data in the form of the law of the wall for a range of Reynolds number. Data for the velocity profiles are in fair agreement with the law of the wall region. For values of  $9 \times 10^3 \leq y^+ \leq 2 \times 10^4$ , the profile data tended to deviate from the law of the wall formulation; this was to be expected since the relation held only for the region  $y_0 \leq y \leq 0.2\delta$ . Data for the submarine model were also in accordance with the law of the wall region and tended to deviate from this formulation for values of  $y \geq 0.2\delta$ .

## WALL SHEAR STRESS

Figure 8 gives distribution results of the hull shear stresses, obtained with the Preston tubes. The variation of the wall shear-stress coefficient is plotted as a function of axial

distance from the bow for various  $U_\infty$ . The seawater shear-stress results given by the Preston tubes agreed with values of  $c_f$  obtained from a solution of the momentum equation given by Granville. As can be seen,  $c_f$  is maximum at the bow and slowly decreases along the hull for a given velocity. No attempt was made to compare the present shear-stress results with the earlier submarine trial results because the earlier data only represented averages over the range of ship speeds. Also, due to the lack of similarity in Reynolds number, the submarine model results could not be compared with the present shear-stress results of the submarine.

The Stanton tube characteristics are presented in Figures 9 and 10. Figure 9 shows the variation of  $\bar{d}_s/d_s$  with  $\tau_w d_s^2/4\rho\nu^2$  for the Stanton tubes, located at  $\ell = 17$  and 136 feet. The quantity  $\bar{d}_s/d_s$  is the ratio of the deviation of the effective center of the Stanton tube from its geometric center  $\bar{d}_s$  to the height of the Stanton tube above the wall  $d_s$  and represents the location of the measurement with respect to the wall. Values of  $\bar{d}_s/d_s$  were calculated from Equation (6) by using the measured values of  $\tau_w$  (Preston tube) and  $\Delta P_s$ . As shown, the values of  $\bar{d}_s/d_s$  become quite large for small values of  $\tau_w d_s^2/4\rho\nu^2$ . The open circles represent previous experimental data for a smooth flat-plate.<sup>19</sup> The difference between the trials and smooth flat-plate data could be attributed to several factors.

1. Roughness effects
2. Differences in Stanton tube geometries
3. Positioning the probes in the laminar sublayer region.

The sensitivity of a typical Stanton tube is shown in Figure 10 for  $\ell = 17$  feet. The results indicate that for a maximum hull shear stress  $\tau_w$  of approximately 2.5 pounds per foot squared, the corresponding Stanton tube differential pressure  $\Delta P_s$  was 0.47 pounds per inch squared.

## CONCLUSIONS

1. The experimental results of the boundary-layer investigation of the full-scale submarine appear to be in agreement with present boundary-layer theory and expectations at high Reynolds number.
2. The submarine full-scale and model velocity profiles agree well with the velocity-similarity laws over a Reynolds number range from  $10^6$  to approximately  $3 \times 10^8$ .
3. Measurements of submarine full-scale, shear-stress distributions are in accordance with predictions of the momentum equation.

---

<sup>19</sup>Souders, W. G., "Application of the Stanton Tube to the Measurement of Wall Shear Stress on a Flat Plate with Polymer Ejection," NSRDC Report 3849 (May 1973).

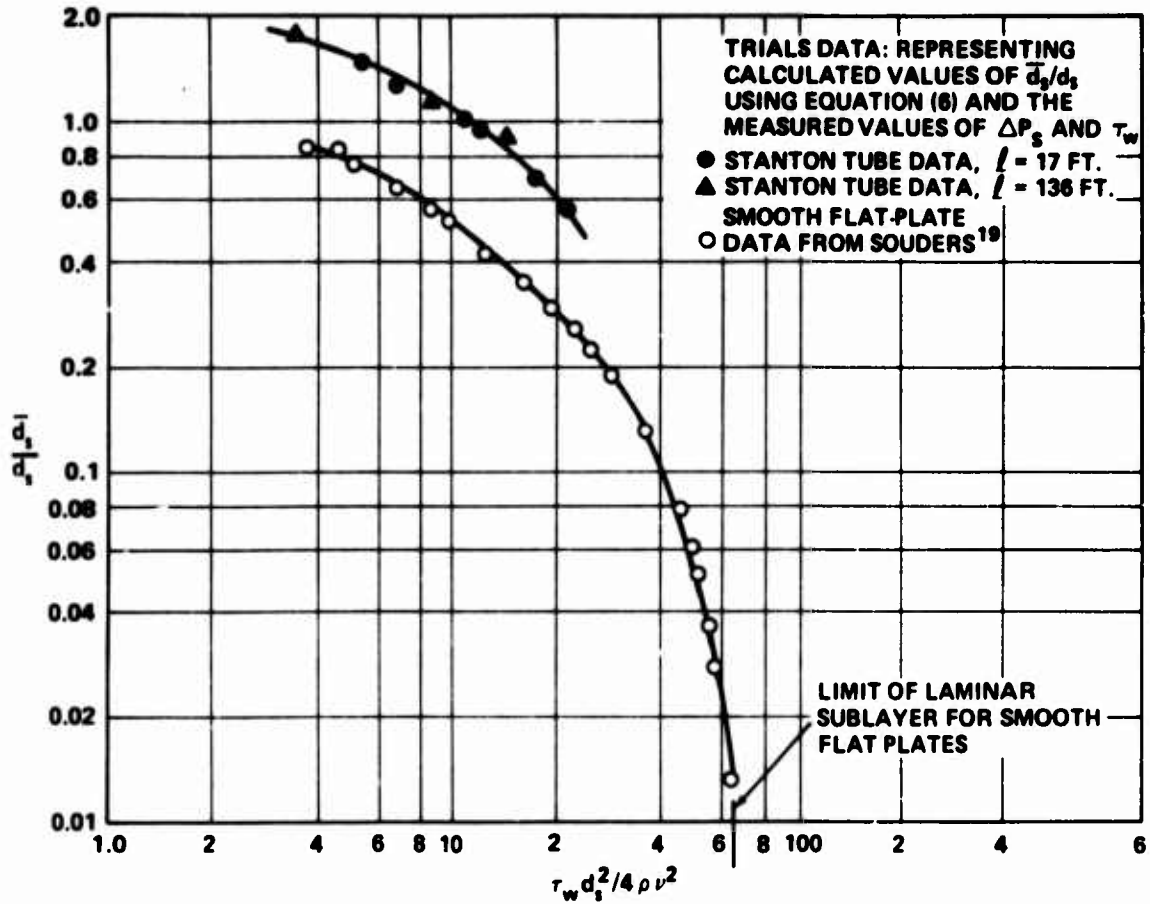


Figure 9 Displacement of Effective Center for Stanton Tubes

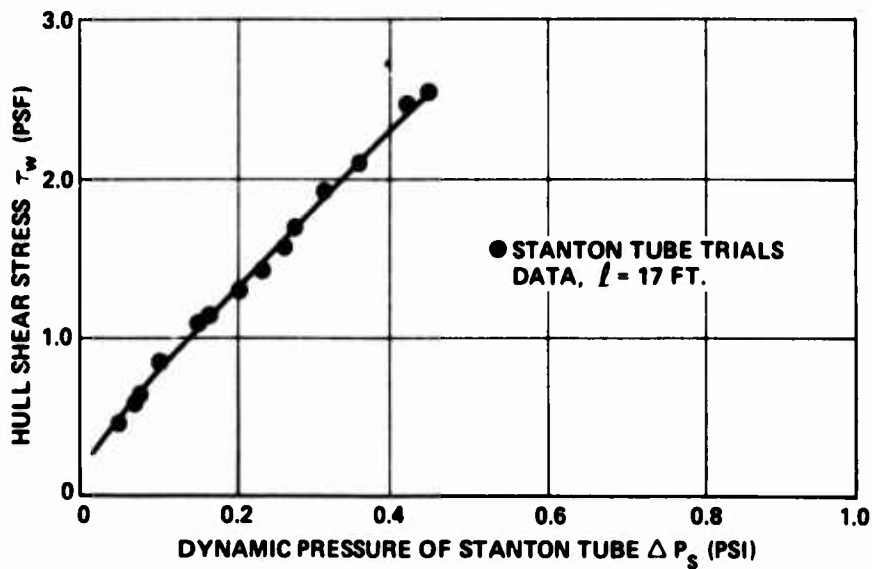


Figure 10 A Typical Stanton Tube Calibration Curve: Variation of Hull Shear Stress as a Function of Stanton Tube Differential Pressure  $l = 17$  Feet

## REFERENCES

1. Hama, F. R., "Boundary-Layer Characteristics for Smooth and Rough Surfaces," *Transactions of the Society of Naval Architects and Marine Engineers*, Vol. 62, p. 333 (1954).
2. Schoenherr, K. E., "Resistance of Flat Surfaces Moving through a Fluid," *Transactions of the Society of Naval Architects and Marine Engineers*, Vol. 40, p. 279 (1932).
3. Schultz-Grunow, F., "New Frictional Resistance Law for Smooth Plates," National Advisory Committee for Aeronautics Technical Memorandum 986 (1941); Translation from *Luft-fahrtforschung* (1940).
4. Granville, P. S., "The Viscous Resistance of Surface Vessels and the Skin Friction of Flat Plates," *Transactions of the Society of Naval Architects and Marine Engineers*, Vol. 64 (1956).
5. von Kármán, T., "On Laminar and Turbulent Friction," National Advisory Committee for Aeronautics TM 1092 (Sep 1946); Translation from *ZAMM* (Aug 1921).
6. Young, A. D. and P. R. Owen, "A Simplified Theory for Streamline Bodies of Revolution and its Application to the Development of High-Speed Shapes," Aeronautical Research Committee (Great Britain) R & M 2071 (Jul 1943).
7. Granville, P. S., "The Calculation of the Viscous Drag of Bodies of Revolution," David Taylor Model Basin Report 849 (Jul 1953).
8. Hinze, J. O., "Turbulence," McGraw-Hill Book Company, Inc., New York (1959).
9. Schlichting, H., "Boundary Layer Theory," McGraw-Hill Book Company, Inc., New York (1960).
10. Preston, J. H., "The Determination of Turbulent Skin Friction by Means of Pitot Tubes," *Journal of the Royal Aeronautical Society*, Vol. 58 (1954).
11. Patel, V. C., "Calibration of the Preston Tube and Limitations on Its Use in Pressure Gradients," *Journal of Fluid Mechanics*, Vol. 23, Part 1, pp. 185-208 (1965).
12. Granville, P. S., "The Determination of the Local Skin Friction and the Thickness of Turbulent Boundary Layers from the Velocity Similarity Laws," *International Shipbuilding Progress*, Vol. 7, No. 69 (1960).
13. Landweber, L. and M. Gertler, "Mathematical Formulation of Bodies of Revolution," David Taylor Model Basin Report 719 (1950).

14. Naval Ship Systems Command, "Preservation of Ships in Service," NAVSHIPS Technical Manual 0901-109-002, Chapter 9090.
15. Daily, J. W. and R. L. Hardison, "A Review of Literature Concerning Impact Probes Used in Steady Flows," Massachusetts Institute of Technology Hydrodynamics Laboratory Report 67, Appendix 1 (Apr 1964).
16. MacMillan, F. A., "Experiments on Pitot-Tubes in Shear Flow," Aeronautical Research Committee Reports and Memoranda 3028 (Feb 1956).
17. Scottron, V. E., "Turbulent Boundary Layer Characteristics over a Rough Surface in an Adverse Pressure Gradient," NSRDC Report 2659 (1967).
18. Head, M. R. and I. Rechneberg, "The Preston Tube as a Means of Measuring Skin Friction," *Journal of Fluid Mechanics*, Vol. 14, Part 1, pp. 1-17 (1962).
19. Souders, W. G., "Application of the Stanton Tube to the Measurement of Wall Shear Stress on a Flat Plate with Polymer Ejection," NSRDC Report 3849 (May 1973).